DESIGN STUDY OF LUMPED INJECTION KICKERS FOR J-PARC MAIN RING

K.Fan, H. Matsumoto, N. Matsumoto, K. Ishii, KEK, 1-1 Oho, Tsukuba, Ibaraki, Japan

Abstract

The injection kicker system of the J-PARC main ring consists of 3 transmission-line type kicker magnets. The system has worked successfully since the initial beam commissioning of the MR. However, the kicker system performance degraded due to the aging of sub-components. In order to meet the requirement for high beam power operation, the upgrade of the injection kicker system is undergoing. Four lumped kickers will be designed to replace the present kickers for their structure simplicity and reliability. To meet the stringent requirement of field rise and fall time, the total inductance of the kicker is crucial. Parameters optimization of the kicker base on 3D simulation has been carried out. This paper presents the study results.

INTRODUCTION

The J-PARC is a high intensity beam facility. The main ring (MR) aims to accelerate proton beam with beam power up to 1 MW. The harmonic number of the MR is nine as shown in Fig. 1. One RF bucket is left empty for the extraction kickers to ease the requirement of field rise time. Four successive batches from the RCS are injected into the MR to fill 8 RF buckets spaced at 300 ns interval.

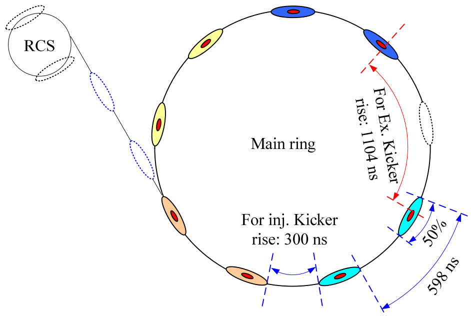

Figure 1: Injection scheme of MR.

The injection system comprises two septa SM1-2, three bump magnets BP1-3 and three kickers K1-3 as shown in Fig. 2. After bending by the injection septa SM1-2, the injected beam approaches the kickers at a small angle of 8.588 mrad. It requires a total kick strength of 0.1096 T.m to deflect the injection beam onto the central orbit. The kicker magnets presently installed at the straight section A are 3 transmission-line type magnets. Two of them are terminated with matched 10 Ω resistors; one kicker is shortened to double the kick strength [1]. Table 1 lists the strength and voltage of each kicker. The kicker system has been used successfully since the start of the beam commissioning. However, the degradation of their performance was observed, which deteriorate the beam quality. The kicker magnet upgrade is needed, however, the power supply will be used continually.

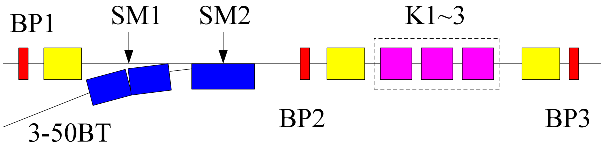

Figure 2: Layout of injection system.

Table 1: Basic parameters of present kickers

Parameters	K1	K2	K3
Angle, mrad	2.053	2.053	4.482
Voltage, kV	52.67	52.67	59

DESIGN CONSIDERATION

The new kickers are designed as four identical matched kicker magnets, which will save cost and ease maintenance. In order to inject beams into the MR without affecting the ‘old’ circulating beams, the maximum time available for both the rise and fall time of the injection kicker is 300 ns as indicated in Fig. 1. Transmission-line kicker can meet the requirement easily. A transmission-line kicker is split in many (n) ‘cells’ to approximately simulate a broadband coaxial cable. The total rise time of the kicker field is given,

$$T_r = t_{in} + t_{fill} \ , \qquad (1)$$

Where t_{in} is the input pulse rise time, t_{fill} is the filling time of a kicker magnet, which is given,

$$t_{fill} = n \cdot \sqrt{L_c \cdot C_c} \ , \qquad (2)$$

Where, L_c and C_c are the inductance and capacitance of a cell respectively. Transmission-line kicker performs much faster than lumped kickers. However, this type of design uses large metal plates to sandwich ferrite cores to construct capacitors making the magnet mechanically complex. Furthermore, the cell inductance is position dependant. In the magnet center, the inductance depends on the core geometry only [2],

$$L_{c1} = \frac{\mu_0 \times w \times l_c}{h} \ , \qquad (3)$$

Where, w and h are the aperture width and height respectively; l_c is the cell length. At the magnet end, the inductance calculation must take into account the fringe field effects. With OPERA 3D code, the inductance of individual cell can be exactly predicted,

$$L_{c2} = \frac{N\Phi_{cell}}{I} \ , \ \Phi_{cell} = \iint B_y ds \ , \qquad (4)$$

Where, N is the number of turns; I is the excitation current; Φ_{cell} is the magnetic flux through the back yoke of the ferrite, as illustrated in Fig. 3.

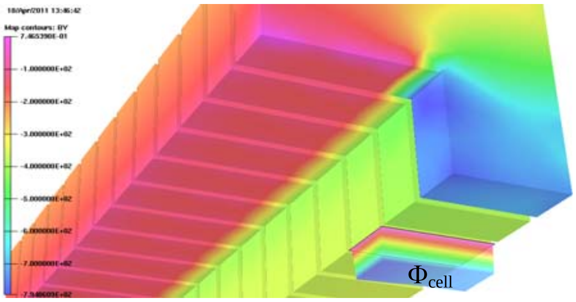

Figure 3: Magnetic flux through back yoke.

Suppose the new kickers are transmission line magnets, and each kicker is 600 mm long composed of the 15 cells, the inductance of individual cell is shown in Fig. 4, which is increasing from the center to the end because of the fringe field. The cell capacitance must be changed accordingly to keep individual cell impedance uniform, which makes difficulties for capacitor construction. Thus, lumped inductance kicker is chosen for the kicker upgrading.

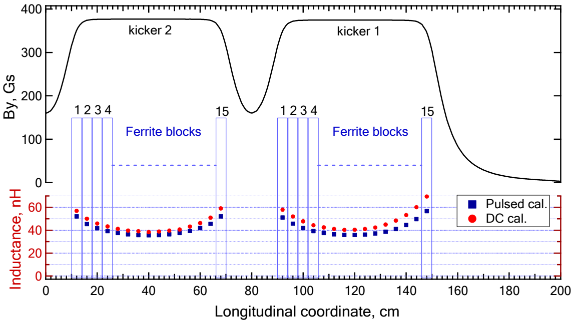

Figure 4: Individual cell inductance (2 kickers).

LUMPED-INDUCTANCE KICKER

Lumped inductance kicker has the advantages of structure simplicity and high reliability. However, the large lumped inductance together with the stray inductance of the circuit limits the rate of rise/fall time of the field, which is exponential with a time constant τ_{lp},

$$\tau_{lp} = \frac{L_m + L_s}{Z}, \qquad (6)$$

Where, L_m and L_s are the kicker inductance and the stray inductance respectively. One of the most important design tasks is to minimize the total inductance.

Choice of Ferrite Material

Ni-Zn ferrite is the best material so far for high-speed kicker design. CMD10 ferrite is chosen as the magnet core, which provides excellent high-frequency response, low core loss. With the beam intensity increase in future, the beam induced kicker heating is a big issue also. CMD10 has very high Curie temperature of 250 ^{o}C.

Magnet Geometry

The cross section of the magnet is shown in Fig. 5. It is window frame structure consists of two "c" shaped ferrite core separated by a copper screen, which plays a role of flux barrier to increase the reluctance of the magnetic path induced by the circulating beam, and thus decrease the flux that couples the circulating beam. The basic kicker dimensions are given in table 2.

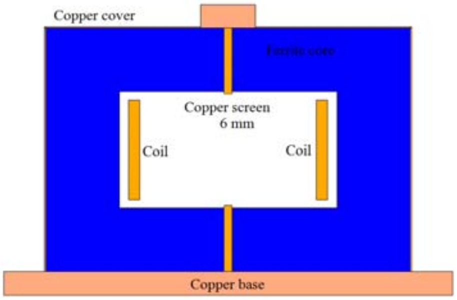

Figure 5: Cross section of kicker magnet.

Table 2: Basic parameters of lumped kicker

Parameters	**Width**	**Height**	**Co. screen**
	130 mm	98 mm	6 mm

Magnet Inductance Optimization

To meet the stringent requirement of field rise/fall time less than 300 ns, the total circuit inductance must be strictly controlled. The measured inductance of the present power supply circuit is about 500 nH. PSPICE simulation shows that the maximum allowable inductance of the magnet coil is limited within 600 nH. The coil has to be split into two coils driven by two separated power supplies. Fig. 6 shows the schematic circuit.

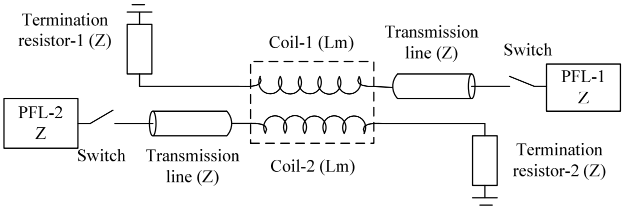

Figure 6: Schematic circuit of kicker system.

There is a competition between required kicker strength and field rise/fall time. 3D simulation shows that, the magnet length should be less than 620 mm to keep its inductance within 600 nH as shown in Fig. 7. In this case, the required power supply voltage is about 66 kV, which closes its maximum capability.

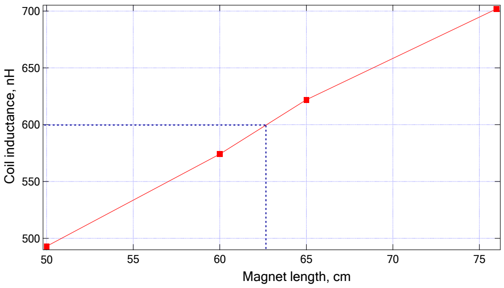

Figure 7: magnet length vs. inductance.

Improvement of Field Waveform

To eliminate the field oscillation due to the mismatched load, a broad band frequency independent load is used, which can be realized by a very circuit as shown in Fig. 8. The load impedance is, (Laplace transform)

$$Z_L = \frac{(Z + sL_m)(Z + 1/sC_m)}{2Z + sL_m + 1/sC_m}, \qquad (7)$$

Where, C_m is the matching capacitance. The circuit is perfectly matched if matching capacitance C_m is,

$$C_m = \frac{L_m}{Z^2}, \qquad (8)$$

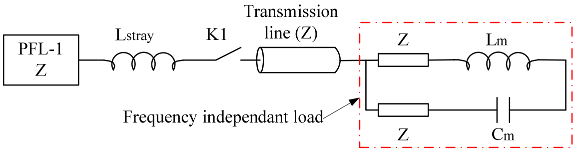

Figure 8: Frequency independent load.

However, a perfect match leads to slow response. The capacitor C_m can be a little mismatch to improve response rate, but small oscillations may occur as shown in Fig. 9. A “tail-bite” [3] circuit can avoid the oscillations.

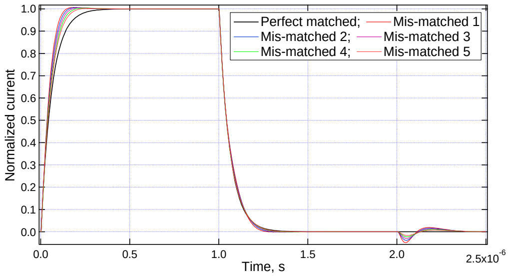

Figure 9: Comparison of circuit response.

Field Quality

The gap field integral uniformity is affected by the fringe field and the copper screen thickness mainly. To asses the entire gap field spacial distribution, 3D particle trajectories are simulated. Consider launching a laminar test beam (81 mm.mrad) parallel to the beam axis as shown in Fig. 10. The beam parameters obtained at the exit include the information of the gap field integral spatial distribution as shown in Fig. 11. Thinner copper screen is preferable in view of gap field uniformity, which leads to a small deviation between beam center and edge.

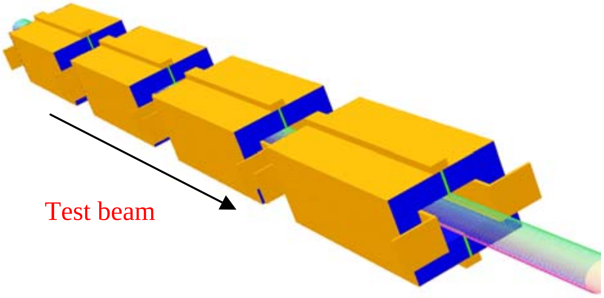

Figure 10: Particle trajectories simulation.

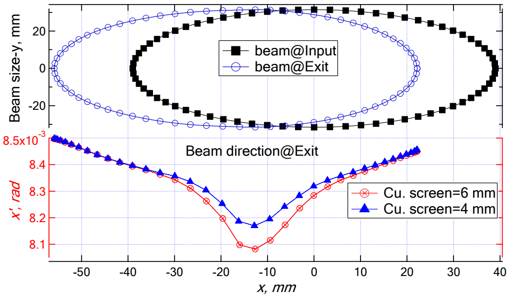

Figure 11: Particle direction after pass through kickers.

Beam Impedance

Power dissipation in the ferrite core may lead to the temperature increase over Curie point particularly for high intensity beam operation. A copper screen can decrease the beam impedance greatly. However, the gap field quality will decrease as indicate in Fig. 11. CST PARTICLE studio is used to evaluate the copper screen thickness effects on the impedance, which is shown in Fig. 12 and Fig. 13.

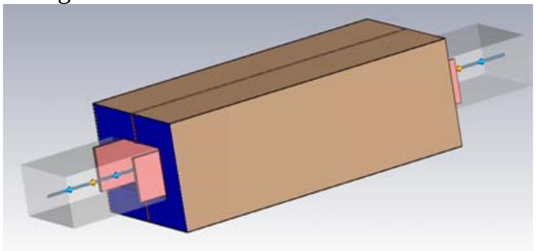

Figure 12: Simulation kicker impedance.

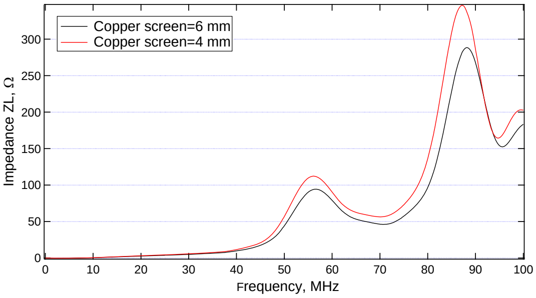

Figure 13: Beam impedance comparison.

FUTURE WORK

Further parameters optimization will continue. Magnet construction, test will be started at the end of this year.

REFERENCES

[1] KEK report 2002-13.

[2] M.J. Barnes, G.D.Wait, Comparison of measured and predicted inductance per cell for a travelling wave kicker magnet.

[3] W. Zhang, W.W. Frey et al, Test modulator of AGS injection fast kicker.